Truncation of Motifs III and IV in Human Lens βA3-Crystallin Destabilizes the Structure†

R. Gupta, K. Srivastava, and O. P. Srivastava*

Department of Vision Sciences, University of Alabama, Birmingham, Alabama 35294-4390

Received March 13, 2006; Revised Manuscript Received June 19, 2006

ABSTRACT: The purpose of our study was to determine the effects of specific truncations on the structural properties of human βA3-crystallin. The following eight deletion mutants of βA3-crystallin were generated: (i) N-terminal extension (NTE) 21 amino acids (βA3[21] mutant), (ii) NTE 22 amino acids (βA3[22] mutant), (iii) NTE (βA3[N] mutant), (iv) NTE plus motif I (βA3[N+I] mutant), (v) NTE plus motifs I and II (βA3[N+I+II] mutant), (vi) NTE plus motifs I and II and connecting peptide (βA3-[N+I+II+CP] mutant), (vii) motifs III and IV (βA3[III+IV] mutant), and (viii) motif IV (βA3 [IV] mutant). The DNA sequencing and MALDI-TOF mass spectrometric methods confirmed desired specific deletions, and the purified mutant proteins exhibited a single band during SDS−PAGE analysis. When ANS bound, all the mutant proteins exhibited fluorescence quenching and a red shift, suggesting that the truncations caused changes in the exposed hydrophobic patches. The CD spectra showed that deletion of either NTE or the N-terminal domain (motifs I and II) had a relatively weaker effect on the structural stability than deletion of the C-terminal domain (motifs III and IV). Intrinsic Trp fluorescence spectral studies suggested changes in the microenvironment of the mutant proteins following truncations. HPLC multiangle light scattering analyses showed that truncation led to higher-order aggregation compared to that in the wild-type protein. Equilibrium unfolding and refolding of WT βA3 with urea were best fit to a three-state model with transition midpoints at 2.2 and 3.1 M urea. However, the two transition midpoints of βA3[21] and βA3[22] and βA3[N] mutants were similar to those of the wild type, suggesting that these truncations had a minimal effect on structural stabilization. Further, the mutant proteins containing the N-terminal domain (i.e., βA3[III+IV] and βA3[IV] mutants) exhibited higher transition midpoints compared to the transition midpoints of the mutant protein with the C-terminal domain (i.e., βA3-[N+I+II+CP] mutant). The results suggested that the N-terminal domain is relatively more stable than the C-terminal domain in βA3-crystallin.

Crystallins (α-, β-, and γ-crystallins) are the major structural proteins of the eye lens. The transparency of the human eye lens depends on the stability and specific interaction among the three crystallins (*1*). The β- and γ-crystallins, derived via gene duplication with a 30% degree of sequence homology, have similar tertiary structures forming a βγ-crystallin superfamily (*1*−*3*). Members of the βγ-crystallin superfamily have a similar core structure, consisting of two homologous globular domains that are connected by an 8−10-amino acid interdomain connecting peptide (CP). However, unlike γ-crystallins, β-crystallins have either an N-terminal extension (in acidic β-crystallins) or both N- and C-terminal extensions (in basic β-crystallins). A family of four acidic and three basic forms of human β-crystallins are encoded by genes that reside on different chromosomes. These exist in vivo as oligomers (*1*) of 50−200 kDa, forming several classes of aggregates: βH (octamers of 160−200 kDa), βL1 (tetramers of 70−100 kDa), and βL2 (dimers of 46−50 kDa).

Studies of cataractous lenses have suggested that the lens opacity is due to protein aggregation and cross-linking that becomes insoluble in lens cells (*4*, *5*). Two major causative factors have been identified for cataract development, i.e., mutations in lens proteins (present at the time of birth) that affect structure, stability, and interactions among crystallins and age-related post-translational modifications of crystallins, (*6*, *7*). Several autosomal dominant cataracts have been identified; few of these are due to mutation in the βA3/A1 or βB1 gene. Burdon et al. showed a splice site mutation at the first base of intron 3 of the CRY βA3/A1 gene segregating with disease that resulted in premature termination of the polypeptide (*8*). A genome-wide search of a five-generation family with autosomal dominant lamellar cataract demonstrated a 3 bp deletion in the CRY BA1/3 gene resulting in G91 deletion in the tyrosine corner (*9*). This study further showed that the deletion resulted in defective folding and a reduction in the solubility of βA3/A1-crystallin, and also in a recombinant βB2 with an identical mutation. In an animal model for a human congenital zonular cataract, the mutation of a T to an A in exon 6 of βA3/A1, affected the formation of the fourth Greek key motif (*10*). Another study

† This study was supported by National Eye Institute Grant EY06400 and partly by NIH Grant P50AT00477 (principal investigator, Dr. Connie Weaver, Purdue University, and subcontract to Dr. Stephen Barnes, University of Alabama).

* To whom correspondence should be addressed: Department of Vision Sciences, Worrell Bldg., 924 South 18th St., University of Alabama, Birmingham, AL 35294-4390. E-mail: srivasta@uab.edu. Phone: (205) 975-7630. Fax: (205) 934-5725.

10.1021/bi060499v CCC: $33.50
Published on Web 07/29/2006

of the autosomal dominant zonular cataract in an Indian family showed the absence of Greek key motifs I and II in βA3/A1 that resulted in a single globular domain, which was segregated with nuclear sutural cataract (*11*). Similarly, a screening of nine Indian families with clinically documented congenital cataract showed that a W151C substitution in exon 6 in the CRYBB2 gene was likely the causative factor (*12*). The hydropathy analysis in this study suggested that increased hydrophobicity of a region with residues 147−155 might impair the solubility of the mutant protein. Another study of the CRYBB2 gene mutant (Q155) caused cerulean cataract, which was due to truncation of 51 residues from the C-terminal region (*13*), and such a recombinant protein exhibited altered biophysical properties (*14*). Together, these studies showed that altered crystallin−crystallin interactions and their conformational changes could lead to cataract development.

The post-translational modifications of crystallins include oxidation, deamidation, and cleavage at a specific site or truncation of terminal extensions. These changes are believed to cause their aggregation and insolubilization leading to cataract development (*15*). Because interactions among β-crystallins to form aggregates in vivo are critical for the maintenance of lens transparency, the truncations might affect their interactions and aggregation. Although the exact interactions among β-crystallins in their oligomeric state are unclear, a previous study (*16*) identified three types of β-crystallin oligomers in human lenses, i.e., β1 (150 kDa, contained βA3/A1-, βA4-, βB1-, and βB2-crystallins), β2 (92 kDa, βA3/A1-, βA4-, βB1-, and βB2- crystallins), and β3 (46 kDa, contained βB1- and βB2-crystallins). The study concluded that the major differences in the oligomers were the presence of βA3/A1- and βA4-crystallins in the β1- and β2-oligomers and their absence in the β3-oligomer, and the aggregate sizes correlated with the length of the N-terminal extension of βB1-crystallin. The βA3/A1- and βB2-crystallins exhibited spontaneous oligomerization into tetramer species in vitro, and NMR studies revealed that the N-terminal extension of βA3-crystallin was exposed to water while the C-terminal region participated in oligomerization (*17*). However, both N- and C-terminal extensions of βB2-crystallin were involved in the protein−protein interactions (*17*). Previous studies have also shown that the deletion of N- and C-terminal extensions of βB1-crystallin had little effect on the stability of oligomers of βB1- and βB2-crystallins (*18*, *19*). A recent study of the crystal structure of a truncated βB1-crystallin suggested that the bulk of the N-terminal extension was not necessary to stabilize its structure but truncation reaching into the N-terminal domain was predicted to cause unfolding and loss of solubility (*20*). Together, these studies suggested that post-translational modifications also affect crystallin−crystallin interactions and could lead to the development of lens opacity.

Age-related truncations of β-crystallins have been reported in bovine (*21*, *22*) and human (*23*−*26*) lenses. In the bovine lenses, βA3 missing 11 and 22 N-terminal extension residues and βB2 and βB3 missing 8 and 22 residues from their N-termini, respectively, were identified (*21*, *22*). Truncations of human lens β-crystallins in aging human lenses occurred mainly at the N-terminal region, i.e., a loss of 49 N-terminal residues in βB1-crystallin (*23*), 5 and 17 N-terminal residues in βB3, and 11 and 21 residues in βA3/A1-crystallin (*24*). Indeed, in the human lenses, the earliest post-translational modifications were the truncation of βB1- and βA3/A1-crystallins (*25*, *26*). Our results also showed that the majority of age-related degradation in human βA3/A1-crystallin occurred at the N-terminal region with a major cleavage site at the $E_{39}-N_{40}$ bond (*27*). Recently, we identified several truncated species of βA3/A1- and βB1-crystallins in human cataractous lenses that were absent in normal lenses (*28*). Together, these reports showed extensive truncation of β-crystallins, which might impair their stability and lead to aggregation.

At present, information regarding the effects of truncations at various sites in β-crystallins on their structural properties is lacking. Recent reports suggest that specific mutations or post-translational modifications could result in an inability of α- or β-crystallins to participate in complex formation (*29*, *30*). It has also been proposed that disruption of β-strands in β-sheets might lead to a loss of subunit interactions among βB2-crystallins (*30*). Because truncation of β-crystallins would lead to the loss of β-strands in β-sheets resulting in abnormal interactions in forming the homo- and heteroaggregates, it might result in poorly soluble protein aggregates and cause cataract development. Therefore, it is important to determine how truncations change the hydrophobic and ionic interactions among β-crystallins, which are required for their proper oligomerization and the transparency of the lens. The purpose of our study was to gain insight into the importance and involvement of specific structural regions (N-terminal extension, motifs, connecting peptide, and domains) of human βA3-crystallin in its stability and protein aggregation. To achieve this, we sequentially deleted βA3-crystallin starting at the N-terminal extension to generate the following eight deletion mutants: (i) N-terminal extension (NTE) 21 amino acids (βA3[21] mutant), (ii) NTE 22 amino acids (βA3[22] mutant), (iii) NTE (βA3[N] mutant), (iv) NTE plus motif I (βA3[N+I] mutant), (v) NTE plus motifs I and II (βA3[N+I+II] mutant), (vi) NTE plus motifs I and II and connecting peptide (βA3[N+I+II+CP] mutant), (vii) motifs III and IV (βA3[III+IV] mutant), and (viii) motif IV (βA3[IV] mutant). Next, we compared the biophysical properties of the eight deletion mutants with wild-type (WT) βA3-crystallin to determine the effects of specific deletions on structural changes and oligomerization and solubility properties. Because the 22 N-terminal residues are cleaved early in life in human lenses, we deleted this region as well as N-terminal residues 1−21 to determine the importance of the former region.

EXPERIMENTAL PROCEDURES

Materials

Restriction endonucleases *Nco*I and *Nde*I, molecular mass protein markers, and DNA markers were purchased from either Amersham Biosciences (South San Francisco, CA) or Promega (Madison, WI). The primers used in the study were obtained from SigmaGenosys (St. Louis, MO). Molecular biology-grade chemicals were purchased from either Sigma or Fisher Scientific unless stated otherwise.

Bacterial Strains and Plasmids

The *Escherichia coli* BL21(DE3) bacterial strain was obtained from Invitrogen (Carlsbad, CA). The human βA3-

Table 1: Oligonucleotide Primers Used for Generation of Deletion Mutants of βA3/A1 Using PCR-Based Mutagenesis

		primers (5′−3′)
WT βA3/A1	forward	CACCATGGAGACCCAGGCTGAGCAGG
	reverse	CTACTGTTGGATTCGGCGAATCGATTG
βA3[21]	forward	CACCCCTACGCCGGGGTCCCTGGGGCCCCCCATG
	reverse	CTACTGTTGGATTCGGCGAATCGATTG
βA3[22]	forward	CACCAACCCTACGCCGGGGTCCCTGGGGCC
	reverse	CTACTGTTGGATTCGGCGAATCGATTG
βA3[N]	forward	CACCTGGAAGATAACCATCTATGATCAG
	reverse	CTACTGTTGGATTCGGCGAATCGATTG
βA3[N+I]	forward	CACCGGCGCCTGGATTGGTTATGAGCAT
	reverse	CTACTGTTGGATTCGGCGAATCGATTG
βA3[N+II+II]	forward	CACCGCTAATCATAAGGAGTCTAAGATG
	reverse	CTACTGTTGGATTCGGCGAATCGATTG
βA3[N+I+II+CP]	forward	CACCTCTAAGATGACCATCTTTGAGAAG
	reverse	CTACTGTTGGATTCGGCGAATCGATTG
βA3[III+IV]	forward	CACCATGGAGACCCAGGCTGAGCAGG
	reverse	CTACTCCTTATGATTAGCTGAACAGAT
βA3[IV]	forward	CACCATGGAGACCCAGGCTGAGCAGG
	reverse	CTATTGTATCTTCATGGAGCCGACTTC

crystallin plasmid DNA in pCRT7/CT TOPO was received from K. Lampi (Oregon Health and Science University, Portland, OR). The gene was excised from the pCRT7/CT plasmid and ligated into a pET100 Directional TOPO vector (Invitrogen) that added an N-terminal six-His tag to the protein. The integrity of the βA31 cDNA was confirmed by DNA sequencing at the DNA Sequencing Core Facility of the University of Alabama. Positive clones were transformed into *E. coli* BL21(DE3) cells. Cells were propagated in Luria Broth, and recombinant bacteria were selected using ampicillin.

Generation of Truncated Mutants of βA3-Crystallin

Recombinant βA3, cloned in the pET100 Directional TOPO vector, was used as a template with specific complementary primer pairs (Table 1) to generate the desired truncated βA3-crystallin mutants. The following regions were deleted using PCR-based mutagenesis: (i) NTE 21 amino acids (βA3[21] mutant), (ii) NTE 22 amino acids (βA31-[22] mutant), (iii) NTE (βA3[N] mutant), (iv) NTE plus motif I (βA3[N+I] mutant), (v) NTE plus motifs I and II (βA3-[N+I+II] mutant), (vi) NTE plus motifs I and II and connecting peptide (βA31[N+I+II+CP] mutant), (vii) motifs III and IV (βA3[III+IV] mutant), and (viii) motif IV (βA3-[IV] mutant). Briefly, 25 ng of template was used under the following PCR conditions: predenaturation at 95 °C for 5 min, followed by 30 cycles of denaturation at 95 °C for 30 s, annealing at 58−60 °C for 45 s (depending on the T_m of the primers), and extensions at 72 °C for 1 min followed by a final extension at 72 °C for 10 min. The PCR products were ligated into the pET100 Directional TOPO vector using the manufacturer's instructions, and the positive clones were identified by restriction analysis using *Nco*I, *Nde*I, and *Sac*I. The DNA sequencing of the selected clones at the DNA Sequencing Core Facility confirmed the desired deletions.

Expression and Extraction of Soluble and Inclusion Body Proteins

E. coli BL21(DE3) pLysS was transformed with mutant amplicons using a standard *E. coli* transformation procedure (*31*). The proteins were overexpressed by addition of IPTG (final concentration of 1 mM), and the cultures were incubated further at 37 °C for 4 h. The cells were harvested and resuspended in lysis buffer [50 mM Tris-HCl (pH 8.0) containing lysozyme (0.25 mg/mL) and protease inhibitor cocktail (Sigma Chemicals)] and homogenized. DNA was degraded using DNase I (10 μg/mL) and incubation on ice for 30 min. The soluble fraction was separated by centrifugation at 8000*g* for 10 min at 5 °C, and the pellet was resuspended in detergent buffer [0.02 M sodium phosphate, 1% (w/v) sodium deoxycholate, 1% NP-40, and 0.02 M Tris-HCl (pH 7.5)]. The detergent-soluble fraction was separated by centrifugation at 5000*g* for 10 min at 5 °C; the pellet was washed with 0.5% Triton X-100, and 10 μg of DNase was added if the pellet was viscous. Washing of the pellet was repeated as necessary to remove bacterial debris from the inclusion bodies. The pellet was resuspended in denaturation buffer [8 M urea, 0.02 M sodium phosphate, and 0.5 M NaCl (pH 7.8) (DB)].

Purification of Wild-Type and Truncated Mutant Proteins

Depending on the nature of the expressed protein (i.e., present in the soluble fraction or in the inclusion bodies), each was purified under either native or denaturing conditions. All purification steps, including refolding of proteins, were carried out at 5 °C unless indicated otherwise. The protein sample obtained as described above was adsorbed on a Pro-bond Ni^{2+} chelating column according to the manufacturer's directions (Invitrogen). During purification under native conditions, the column was loaded with the protein sample followed by washing with native buffer [20 mM sodium phosphate (pH 7.8) containing 0.5 M NaCl and 10 mM imidazole (NB)] and finally eluted with NB containing 250 mM imidazole (pH 7.8). During purification under denaturing conditions, the column was equilibrated with DB. The protein sample was applied, and unbound proteins were eluted first with DB followed by a second wash with DB (pH 6.0) and a third wash with DB (pH 5.3). The bound proteins were eluted with DB containing 250 mM imidazole (pH 7.8).

SDS−PAGE analysis (*32*) was used to identify the fractions containing the desired purified protein during purification under either native or denaturing conditions. The fractions purified under native conditions were pooled, dialyzed against 0.05 M phosphate buffer (pH 7.5) at 5 °C, and stored at −20 °C until they were used. The proteins

purified under denaturing conditions were refolded using a previously published method as described below.

Refolding of Mutant Proteins Purified under Denaturation Conditions

A previously published protein refolding method was used (*9*). The βA3 species, purified under denaturing conditions, were dialyzed overnight against 25 mM Tris (pH 7.2) containing 6 M urea and 1 mM DTT with three changes of buffer. The denatured protein was refolded into a urea-free buffer. Briefly, the refolding was carried out by adding dropwise an excess of a cold (1:100), stirred refolding buffer [25 mM Tris-HCl and 1 mM DTT (pH 7.2)] using a stirred ultrafiltration cell (Millipore). Circular dichroism spectral analysis was performed to compare structures of the refolded proteins to that of WT protein as described below.

The purity of WT βA3-crystallin and the mutant proteins was examined by SDS−PAGE. The MALDI-TOF mass spectrometric analysis of the purified proteins was performed at the Mass Spectrometric Facility of the University of Alabama at Birmingham to confirm the desired deletions. The protein concentrations were determined by either using the Pierce protein determination kit or determining the absorbance at 280 nm and utilizing extinction coefficients of individual proteins. Extinction coefficients were derived from corresponding amino acid sequences of a protein using http://www.expasy.org/cgi-bin/protparam. All the biophysical measurements were carried out with His-tagged proteins.

Determination of Structural Properties of WTβA3 and Its Mutant Proteins

ANS Binding and Fluorescence Spectroscopy. The binding of a hydrophobic probe, 8-anilino-1-naphthalenesulfate (ANS), to WT βA3 and the mutant proteins was assessed by recording fluorescence spectra with excitation at 390 nm and emission between 400 and 600 nm as described previously (*31*). In these experiments, 15 μL of 0.8 mM ANS (dissolved in methanol, final concentration of 12 μM) was added to protein preparations [0.15 mg/mL, dissolved in 10 mM sodium phosphate buffer (pH 7.4) containing 100 mM NaCl] and incubated for 10 min at 37 °C.

Circular Dichroism Studies. The CD spectra of WT βA3 and mutant proteins were determined using a JasCo model 62DS spectropolarimeter at room temperature as described previously (*31*). The protein preparations at 0.3 mg/mL in 50 mM potassium phosphate buffer (pH 7.4) with a path length of 1 mm were used for recording the far-UV CD spectra. The reported spectra are the average of five scans, corrected for buffer blank, and were smoothed. The β-sheet contents of WT and its truncated mutant proteins were determined on the basis of the CD spectra using PROSEC.

Intrinsic Trp Fluorescence Emission Spectra. All fluorescence spectra were recorded in corrected spectrum mode using a Shimadzu RF-5301PC spectrofluorophotometer with excitation and emission slit widths of 10 nm. The intrinsic Trp fluorescence intensities of WT βA3 and the mutant proteins (at 10 μg/mL) were recorded using an excitation wavelength of 295 nm and emission between 300 and 400 nm. First, the spectra were recorded under native conditions after dialysis of protein preparations against an unfolding−refolding buffer [10 mM sodium phosphate buffer, 5 mM DTT, and 1 mM EDTA (pH 7.4) (UR buffer)]. Next, each sample was dialyzed against UR buffer containing 9 M urea, and fluorescence spectra under denaturing conditions were recorded as described above.

Oligomer Size Determination by Dynamic Light Scattering. A multiangle laser light scattering instrument (Wyatt Technology, Santa Barbara, CA) coupled to a HPLC system was used to determine the absolute molar mass of the WT protein and its truncated mutant proteins. Briefly, protein samples in 50 mM sodium phosphate (pH 7.4) were filtered through a 0.2 μm filter prior to being analyzed. Results used 18 different angles, and the angles were normalized with the 90° detector.

Equilibrium Unfolding and Refolding. To study the stability of WT βA3-crystallin and its mutant proteins, urea-induced unfolding and refolding were assessed according to methods described previously (*9*, *33*, *34*). For an unfolding equilibrium, purified WT βA3 or the mutant proteins were diluted to 10 μg/mL in increasing concentrations of urea between 0 and 9 M in UR buffer. The protein samples were incubated at 37 °C for 24 h to ensure that equilibrium was reached. For the refolding experiments, different protein samples (100 μg) were denatured in 9 M urea in UR buffer for 24 h at 37 °C. The protein was subsequently refolded by dilution of proteins to 10 μg/mL with the urea concentration decreasing from 9 to 0.9 M. The refolding samples were incubated at 37 °C for 24 h to reach equilibrium.

Fluorescence emission spectra were recorded for each sample during unfolding and refolding as described above, and the spectra were corrected for the buffer signal. The ratios of emission intensities of 360 to 330 nm (fluorescence at 360 to 330 nm) against urea concentration were plotted to analyze the results. Equilibrium unfolding and refolding data were fit either to a two-state or to a three-state model using the Kaleidagraph (Synergy Software) curve fitting function, and the transition midpoints were calculated from these fits.

Molecular Modeling for Three-Dimensional Structures. Because the three-dimensional structure of βA3 is at present unknown, computational methods for assessing the βA3/A1 protein structure were attempted on the basis of its amino acid sequence and sequence homology as described previously (*12*). The proteomics tools of ExPasy Server (http:/www.expasy.org/cgi-bin/niceprot and http://swiss model.expasy.org) were used. On the basis of a Blast search, manual verification in clustalX (www.ebi.ac.UK/clustalw) between human βA3 and βB1, which were 48.5% identical, and using the coordinates from PDB entry 1OKI of truncated βB1-crystallin, human βA3 was modeled with the help of S. Narayana and M. Carson of the Center for Biophysical Sciences and Engineering at the University of Alabama at Birmingham.

RESULTS

Confirmation of Site-Specific Deletions in βA3/A1 Mutant Proteins

Human βA3-crystallin has 215 amino acids, which are organized in two domains; each domain contains two Greek key motifs. The N-terminal domain (residues 1−118) and the C-terminal domain (residues 124−215) are connected via a connecting peptide (CP, residues 119−123), and the

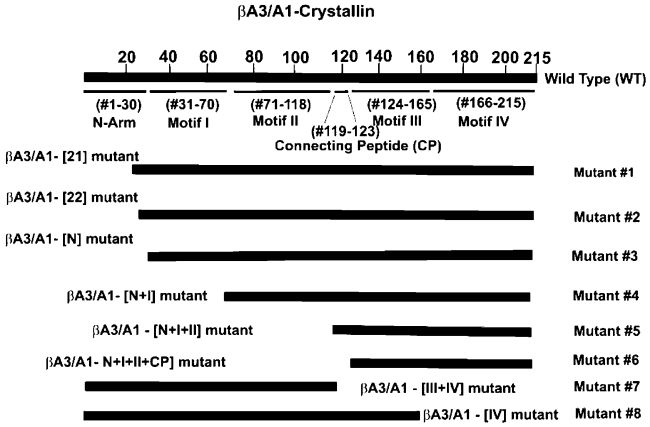

FIGURE 1: Schematic diagram showing the regions and residue numbers forming the N-terminal extension, motif I, motif II, connecting peptide, motif III, and motif IV. In the eight deletion mutants (identified by their names at the left), the residue numbers identified in parentheses were deleted. The deletions were carried out starting from the N-terminal region (i.e., first 21 or 22 N-terminal residues or the entire N-terminal extension followed by motif I, motif II, connecting peptide, motif III, and motif IV).

protein also has an N-terminal extension (NTE, residues 1−30). Deletions of NTE or each of the four motifs one at a time were achieved using the PCR-based mutagenesis method (Figure 1). The deletions were confirmed by DNA sequencing in the coding sequence and by the MALDI-TOF mass spectrometric methods in the expressed proteins. Analyses of the mass of tryptic fragments of each of the mutant proteins compared to WT protein (Figure 2A−C) confirmed their specific desired deletions. Panels B and C of Figure 2 show the representative MALDI-TOF spectra of tryptic fragments of two mutant proteins, i.e., βA3[22] mutant and βA3[IV] mutant proteins. As shown in Figure 2B, the tryptic fragment with a mass of 1611.82 Da (residues 33−45) confirmed the deletion of 22 N-terminal amino acids. Further, the presence of tryptic fragments with masses of 1484.75 Da (residues 126−137) and 1727.85 Da (residues 197−211) in the βA3[22] mutant protein suggested the intact C-terminus was present in the mutant protein as inWT βA3. Similarly, the tryptic fragments with a masses 1611.8 Da (residues 33−45), 2278.99 Da (residues 46−64), and 2295.5 Da (residues 91−109) were observed in the βA3[IV] mutant protein (Figure 2C). Additionally, the absence of C-terminal tryptic fragment peaks with a mass of 1484.65 Da (residues 126−137) and 1727.71 Da (residues 197−211) compared to the WT βA3 protein confirmed the deletion of motif IV. Similar determinations of the masses of tryptic fragments by MALDI-TOF confirmed specific deletions in the six remaining mutant proteins.

Expression of WT βA3 and Mutant Proteins in the Soluble Fraction and/or Inclusion Bodies

The expression of WT βA3 and its eight deletion mutant proteins was induced in BL21(DE3) cells using 1 mM IPTG for 4 h. While the WT protein was recovered in the soluble fraction of *E. coli* cells, few mutant proteins (i.e., βA3[21] mutant, βA3[22] mutant, βA3[N] mutant, and βA3[III+IV] mutant) were found in both the soluble fraction and inclusion bodies, whereas the remaining mutant proteins (i.e., βA3-[N+I] mutant, βA3[N+I+II] mutant, βA3[N+I+II+CP]

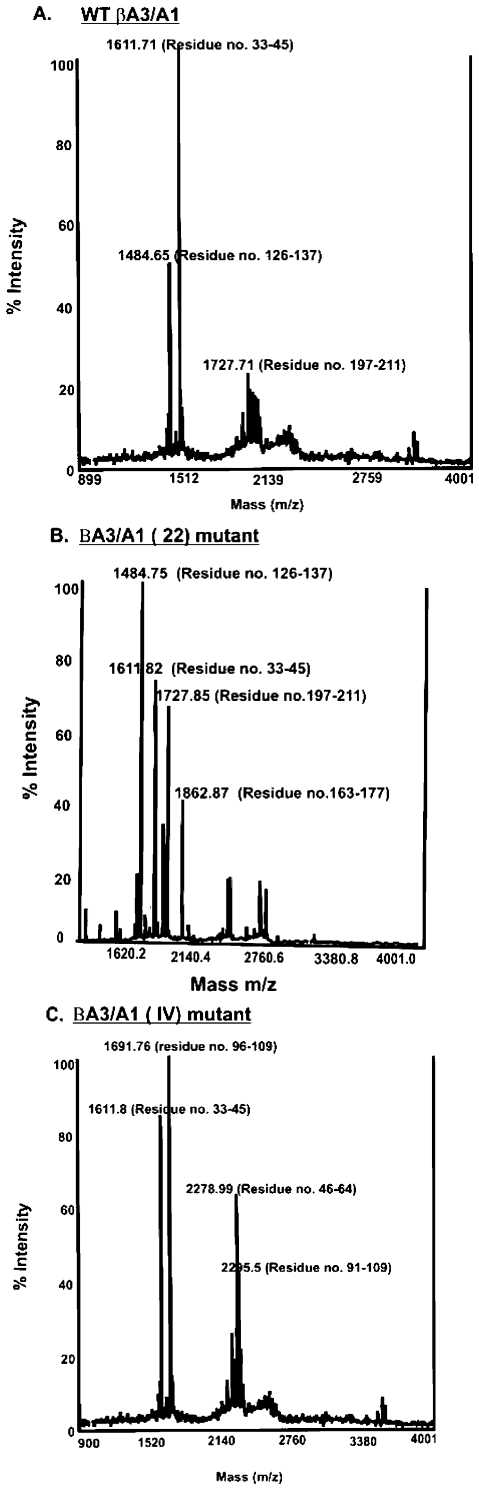

FIGURE 2: MALDI-TOF analysis of tryptic fragments of (A) WT βA3, (B) βA3[22] mutant protein, and (C) βA3[IV] mutant protein. (A) Tryptic fragments with masses of 1611.71 (residues 33−45) and 1727.71 Da (residues 197−211) confirmed the full-length protein. (B) Tryptic fragment with a mass of 1611.82 Da (residues 33−45) confirmed the deletion of 22 N-terminal amino acids. The presence of tryptic fragments with masses of 1484.75 (residues 126−137) and 1727.85 Da (residues 197−211) in the βA3[22] mutant protein suggested an intact C-terminus in the mutant protein like that in WT βA3. (C) The absence of C-terminal tryptic fragments peaks with masses of 1862.87 (residues 163−177) and 1727.71 Da (residues 197−211) in the βA3[IV] mutant protein compared to the WT βA3 protein and βA3[22] mutant protein confirmed the deletion of motif IV. Similar determinations of the masses of tryptic fragments by MALDI-TOF confirmed specific deletions in the six remaining mutant proteins (data not shown).

Table 2: Presence of WT βA3-Crystallin and Its Deletion Mutant Proteins in Soluble Fractions and/or Inclusion Bodies

crystallin species	soluble fraction	inclusion bodies
WT βA3	+	−
βA3[21]	+	+
βA3[22]	+	+
βA3[N]	+	+
βA3[N+I]	−	+
βA3[N+I+II]	−	+
βA3[N+I+II+CP]	−	+
βA3[III+IV]	+	+
βA3[IV]	−	+

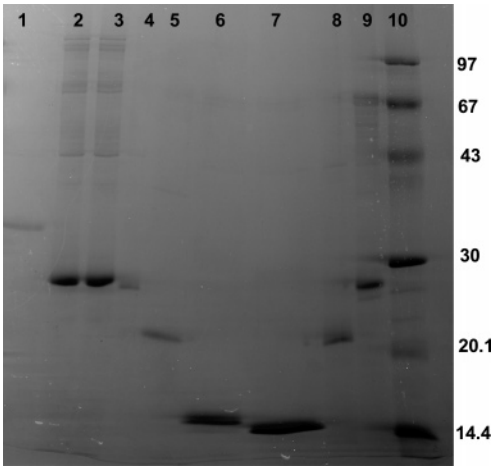

FIGURE 3: SDS−PAGE analysis of purified WT βA3 and its eight truncated mutant proteins following their purification. Purification of protein species was performed by Ni^{2+} affinity chromatography as described in Experimental Procedures: lane 1, WT βA3 protein; lane 2, βA3[21] mutant; lane 3, βA3[22] mutant; lane 4, βA3[N] mutant; lane 5, βA3[N+I] mutant; lane 6, βA3[N+I+II] mutant; lane 7, βA3[N+I+II+CP] mutant; lane 8, βA3[III+IV] mutant; lane 9, βA3[IV] mutant and lane 10, molecular weight marker.

mutant, and βA3[IV] mutant) were exclusively present only in the inclusion bodies (Table 2).

Purification of WT βA3 and Mutant Proteins

WT βA3 and the mutant proteins were overexpressed at 37 °C in *E. coli* and purified to homogeneity using the Ni-Probond affinity column as described in Experimental Procedures. Because of the high-affinity binding of the N-terminal six-His tag of the proteins to Ni-Probond chelating resin, the purification of the WT and eight mutant proteins was easier and less time-consuming. WT βA3-crystallin, present in the soluble fraction, was purified under native conditions, and the inclusion body-associated proteins were purified under denaturing conditions. In some cases, the imidazole-eluted protein fraction from the affinity column was dialyzed to remove imidazole and urea and rechromatographed as described above through the Ni-Probond affinity column. Following purification, the WT and mutant proteins exhibited single bands during SDS−PAGE analysis, and their molecular masses ranged between 14 and 30 kDa depending on their deletion sites (Figure 3). The six His tags (molecular mass of His = 137 Da) increased the molecular mass of each species by 800 Da. Because some of the truncated mutant proteins were purified from the inclusion bodies under denaturing conditions, they were refolded in the native state as described in Experimental Procedures. However, these

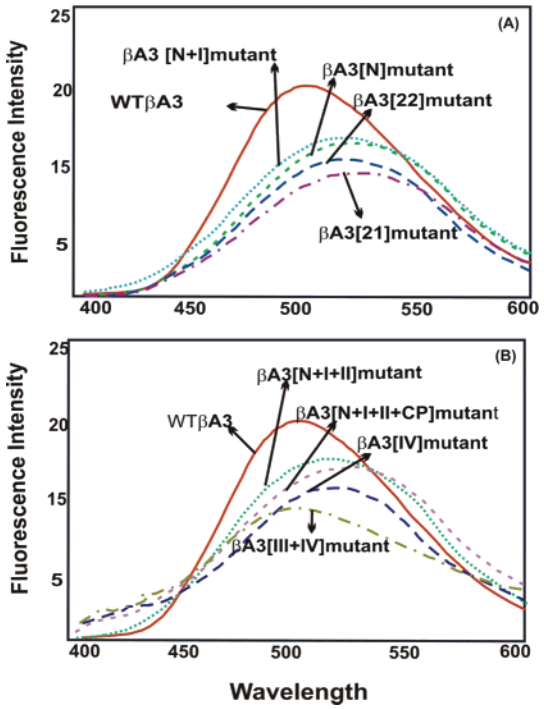

FIGURE 4: Fluorescence spectra of WT βA3 and its eight deletion mutant proteins after ANS binding. In these experiments, 15 μL of 0.8 mM ANS (dissolved in methanol, final concentration of 12 μM) was added to protein preparations [0.15 mg/mL, dissolved in 10 mM sodium phosphate buffer (pH 7.4) containing 100 mM NaCl] and the mixture incubated for 10 min at 37 °C. The fluorescence spectra were recorded with excitation at 390 nm and emission between 400 and 600 nm.

proteins could not be concentrated beyond the following specific concentrations: 0.27 mg/mL for the βA3[21] mutant, 0.3 mg/mL for the βA3[22] mutant, 0.27 mg/mL for the βA3-[N] mutant, 0.31 mg/mL for the βA3[N+I] mutant, 0.473 mg/mL for the βA3[N+I+II] mutant, 0.372 mg/mL for the βA3[N+I+II+CP] mutant, 0.481 mg/mL for the βA3-[III+IV] mutant, and 0.32 mg/mL for the βA3[IV] mutant. Together, the results suggested that the lower solubility of the purified mutant proteins compared to that of the WT βA3 species was consistent with their presence in the inclusion bodies.

Comparison of Properties of WT βA3-Crystallin and Its Eight Truncated Mutant Proteins

Surface Hydrophobicity. Lens β- and γ-crystallins fold into an N-terminal domain consisting of Greek key motifs I and II, and a similar C-terminal domain containing Greek key motifs III and IV (*35*). Each Greek key motif contains four consecutive β-strands that intercalate to form two β-sheets (*36*). The human γD-crystallin structure [X-ray crystal structure determined at 1.25 Å (*37*)] contains a central hydrophobic cluster and polar peripheral pairwise interactions surrounding the cluster. Because of the similarity between β- and γ-crystallins, truncation of these crystallins would affect the central hydrophobic cluster. To investigate the effects of truncations on surface hydrophobicity and the solvent-exposed nonpolar surfaces, the bindings of ANS to WT βA3 and its truncated mutant proteins were compared. Each protein bound to ANS and exhibited quenching in its fluorescence intensity (Figure 4A,B). Among these, the

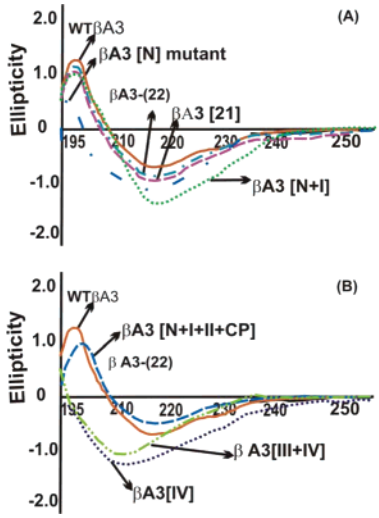

FIGURE 5: Far-UV CD spectra of WT βA3 and its eight deletion mutant proteins. The protein preparations (0.3 mg/mL) were in 50 mM potassium phosphate buffer (pH 7.4), and a path length of 1 mm was used for recording the far-UV CD spectra. The reported spectra are the average of five scans, corrected for buffer blank, and were smoothed.

following decreasing order of fluorescence intensity was observed: WT βA3 > βA3[N+I+II] mutant > βA3[N+I] mutant > βA3[N] mutant > βA3[N+I+II+CP] mutant > βA3[IV] > βA3[22] mutant > βA3[III+IV] mutant > βA3-[21] mutant. The results suggested a higher level of exposure of the hydrophobic patches in the truncated proteins than in the WT protein. Proteins with truncation of the N-terminal extension (i.e., in the [21], [22], and [N] mutant proteins) did exhibit relatively reduced fluorescence intensity and a red shift from 505 to 530 nm. Similarly, the truncation of motifs I and II (i.e., in βA3[N+I] and βA3[N+I+II] mutant proteins) resulted in relatively less quenching than that with only the N-terminal truncation, but a red shift from 505 to 530 nm was observed. The red shift suggested an increased level of exposure of the hydrophobic patches. The proteins with truncation of either only motif IV or both motifs III and IV showed maximum quenching relative to any other truncated mutant proteins, but former proteins showed a red shift from 505 to 520 nm, suggesting an increased accessibility of the hydrophobic patches (Figure 4A,B). Together, the results suggested that the truncation in βA3-crystallin resulted in an altered native hydrophobic core environment, and the relative differences in the levels of quenching with red shifts suggested that their microenvironments were not identical. The variation in quenching and red shifts might be due to differences in their tertiary structures following truncations of different regions.

Circular Dichroism Spectra. To evaluate the effect of specific truncations on secondary structural changes in the mutant proteins, far-UV circular dichroism (CD) spectra were determined (Figure 5). As described in Experimental Procedures, some of the mutant proteins were purified under denaturing conditions and were refolded prior to determination of the CD spectra. As previously reported (*33*), the CD spectra of WT βA3 displayed a minimum at 218 nm, suggesting that the protein is mostly in β-sheet conformation and is properly folded. The truncated mutants exhibited varied spectra (Figure 5A,B). The truncation up to the N-terminal extension showed a spectrum similar that of WT βA3-crystallin, suggesting mostly β-sheet content. On the basis of secondary structure prediction using PROSEC on the CD signal, the β-sheet contents of WT βA3, βA3[21], βA3[22], and βA3[N] mutants were ~63%. The truncation of motifs I, II, and CP (i.e., residues 1−123) resulted in a spectrum with a content of β-strand structure greater than that of the WT protein and lacking a signal in the range of 220−230 nm, which was likely due to loss of Trp side chains. The β-sheet contents for βA3[N+I], βA3[N+I+II], and βA3[N+I+II+CP] mutant proteins were between 73 and 75%. These results are consistent with the loss of two buried Trp residues (at positions 73 and 99) and two partially buried Trp residues (at positions 31 and 99) following truncation of motifs I, II, and CP in the mutant protein (*33*). The mutant proteins with truncation of motifs III and IV (residues 124−215) exhibited spectra with λ_{max} values between 205 and 208 nm, suggesting largely unfolded polypeptides, although they were not random coil compared to the WT βA3 protein. These two mutants also lacked the two buried Trp residues (at positions 168 and 198) and a partially buried Trp residue (at 195 position). However, apparently truncation of motifs III and IV had deleterious effects on structural stability. Previously, the deletion of the "G" residue at position 91 produced a polypeptide relatively more unfolded than WT βA3-crystallin (*9*). Therefore, it appears that both genetic defect, associated with human inherited cataract (*11*−*13*), and post-translational truncations occurring in vivo have similar consequences with respect to βA3 structure. The significant change in secondary structure might explain a part of the mechanism that leads to defective folding and poor solubility that result in protein aggregation during cataract development.

Determination of the Molecular Mass of WT βA3 and Its Truncated Mutants. To determine whether the truncations affect their ability to dimerize or oligomerize, HPLC multiangle light-scattering (MALS) analysis of WT βA3 and its truncated mutant proteins was performed. Compared to WT protein, truncation of 21 N-terminal amino acids (βA3-[21] mutant), 22 N-terminal amino acids (βA3[22] mutant), or the entire N-terminal extension (βA3[N] mutant) resulted in aggregates with masses of 259−267 kDa. Truncation of both the N-terminal extension and motif I (βA3[N+I] mutant) resulted in aggregates with a mass of 621 kDa, whereas truncation of motifs I and II (βA3[N+I+II] mutant), motifs I and II and connecting peptide (βA3[N+I+II+CP] mutant), motifs III and IV (βA3[III+IV] mutant), and motif IV (βA3[IV] mutant) resulted in aggregates with masses ranging between 1096 and 2592 kDa. The data suggested these higher-order aggregates could be due to nonspecific aggregation.

Intrinsic Fluorescence Spectra. βA3-Crystallin contains a total of nine Trp residues (*33*), of which four are buried (73, 99, 168, and 198), three partially buried (31, 96, and 195), and two exposed (139 and 153). Because each of the two domains contains two buried Trp residues in its hydrophobic core, these four Trp chromophores could be used as probes to monitor changes in the tertiary structures of the protein following truncations. The intrinsic fluorescence emission spectra of WT βA3 and its mutant proteins were compared following excitation at 295 nm and emission between 300 and 400 nm. The WT βA3-crystallin under

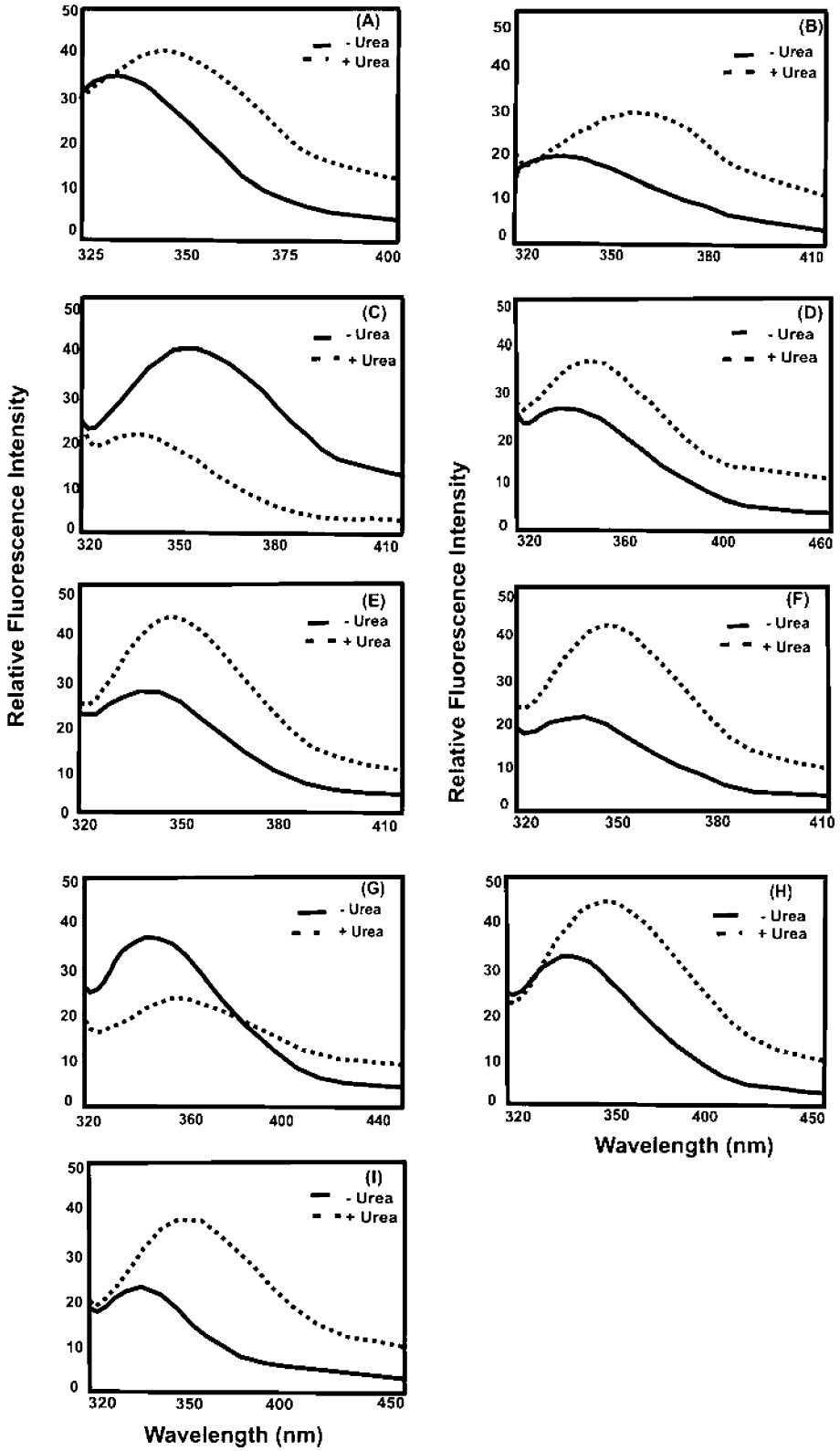

FIGURE 6: Intrinsic Trp fluorescence spectra of native and denatured βA3 and its eight truncated mutant proteins. The protein preparations (10 μg/mL) were excited at 295 nm, and emission spectra were recorded between 300 and 400 nm. First, the spectra were recorded under native conditions after dialysis of protein preparations against an unfolding−refolding buffer [10 mM sodium phosphate buffer, 5 mM DTT, and 1 mM EDTA (pH 7.4) (UR buffer)]. Next, each sample was dialyzed against the UR buffer containing 9 M urea, and fluorescence spectra were recorded as described above: (A) WT protein, (B) βA3[21] mutant, (C) βA31[22] mutant, (D) βA3[N] mutant, (E) βA3[N+I] mutant, (F) βA3[N+I+II] mutant, (G) βA3[N+I+II+CP] mutant, (H) βA3[III+IV] mutant, and (I) βA3[IV] mutant.

native conditions exhibited an emission maximum of 332 nm, which was typical of the four inaccessible (buried) Trp residues to a solvent in the hydrophobic core of the molecule (Figure 6). In contrast, the fluorescence maxima for the truncated mutant proteins under native conditions exhibited a red shift, which ranged between 333 and 342 nm (Figure

Table 3: Fluorescence Emission Maxima of WT βA3 and Its Deletion Mutants under Native and Denaturing Conditions following Excitation at 295 nm

crystallin species	native (nm)	denaturing (nm)
WT βA3/A1	332	349
βA3[21]	337	356
βA3[22]	338	354
βA3[N]	333	349
βA3[N+I]	341	351
βA3[N+II]	340	352
βA3[N+II+CP]	342	354
βA3[III+IV]	340	353
βA3[IV]	339	354

6 and Table 3). Further, compared to that of the WT protein, the fluorescence emission of almost all the mutant proteins (i.e., in βA3[21], βA3[N+I], βA3[N+I+II], βA3[N], βA3-[III+IV], and βA3[IV] mutant proteins) under the native condition showed quenching with the exception of βA3[22] and βA3[N+I+II+CP] mutant proteins. The results suggested, following deletions, an altered microenvironment and tertiary structures in the mutant proteins.

The urea-denatured WT protein exhibited the highest fluorescence emission at ~349 nm, which was similar to the data previously reported for the non-His-tagged βA3 protein (*9*). The urea-denatured mutant proteins exhibited emission maxima between 349 and 356 nm (Table 3). Under denaturing conditions, the mutant proteins exhibited increased fluorescence intensity and a red shift in λ_{max} except in βA3-[22] and βA3[N+I+II+CP] mutant proteins, which exhibited fluorescence quenching compared to the WT βA3 protein (Figure 6).

Fluorescence Emission Spectra with Unfolding of WT βA3-Crystallin and Truncated Mutant Proteins. To determine whether all nine Trp residues (including the four that are buried) of βA3-crystallin were completely exposed during urea denaturation, the fluorescence emission spectra of the WT and mutant proteins were determined at varying urea concentrations. Fluorescence emission spectra of WT protein exhibited a red shift as the maximum fluorescence wavelength increased from 332 to 349 nm, indicating protein unfolding (Figure 7). The results suggested that in the denatured state, the paired and buried Trp in each of the two domains of the WT protein were less quenched compared to those after exposure of the protein to an aqueous environment. As shown in Figure 7, a complete denaturation of the WT protein occurred at ≥7 M urea. The mutant proteins also exhibited complete denaturation in ≥7 M urea with a red shift (data not shown).

Equilibrium Unfolding and Refolding and Stability of WT βA3/A1-Crystallin

A previous study has compared the denaturation of βA3 and its stability with those of other β-crystallins and β-crystallin heteroaggregates (*33*). However, detailed equilibrium protein unfolding and refolding of βA3-crystallin remain unexplored. We carried out a detailed examination of unfolding and refolding of WT βA3 and its eight truncated mutant proteins with the rationale that information will provide a correlation between truncation and protein stability, including solubility. The results might also serve as a model system for other β-crystallins, providing information regarding their in vivo stability and aggregation following truncation.

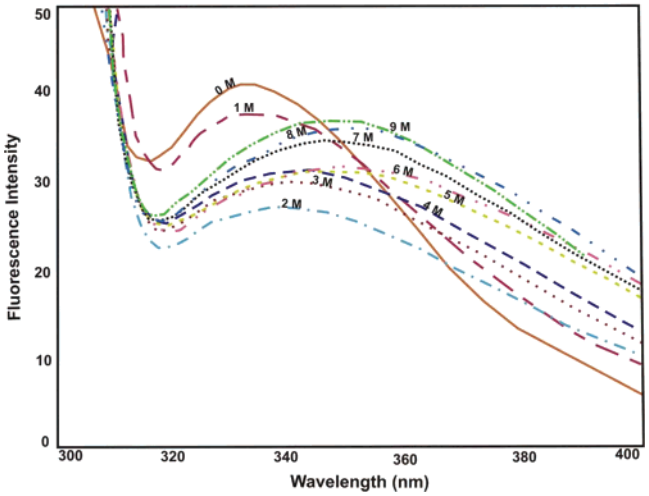

FIGURE 7: Representative urea-induced (from 0 to 9 M) denaturation of WT βA3-crystallin measured by Trp fluorescence spectroscopy. The protein concentration was 10 μg/mL, and the fluorescence emission was measured from 300 to 400 nm with excitation at 295 nm. Similar urea-induced denaturation of the eight βA3 deletion mutant proteins was also performed (data not shown).

To monitor the unfolding and refolding simultaneously, the ratio of fluorescence intensities at 360 and 330 nm (FI_{360}/FI_{330}) was plotted as a function of urea concentration. Equilibrium unfolding or refolding of WT βA3 was recorded for the first time, although such studies have been carried out with basic β-crystallins (*38*, *39*) and γD-crystallins (*34*, *40*). When WT βA3-crystallin was allowed to equilibrate at 37 °C for 20 h, it exhibited a single major unfolding transition midpoint. The refolding transition appeared to be reversible in at >2 M urea. When the denatured protein was incubated with the decreasing urea concentrations, the high-molecular mass aggregates, as demonstrated by increased FI, were observed at <2 M urea (Figure 8A). The data from WT βA3 were fitted to either a two-state or a three-state model. In the case of the WT protein, the two-state model yielded unfolding and refolding transition midpoints of 3.18 and 2.8, respectively. However the same data when fitted to a three-state model yielded a transition midpoint of 2.4 from the native to an intermediate and a midpoint of 2.2 from an intermediate to the unfolded transition. Since the two domains of WT βA3 associate to form a dimer, it was likely that a three-state model was a better fit of the data. Previously, the urea denaturation curve for βA3/A1-crystallin has shown a midpoint at 3.4 M urea (*33*). However, this study did not attempt to fit the data to either a two-state or a three-state model. The data from the equilibrium unfolding and refolding of all the truncated mutants were fitted to a three-state model. The transition 1 (native to an intermediate) and transition 2 (intermediate to an unfolded transition) midpoints of all the mutants are listed in Table 4. In order to determine the stability of N- and C-terminal domains, the unfolding process in different mutant proteins primarily based on transition-2 were compared to WT protein.

The βA3[21], βA3[22], and βA3[N] mutant proteins exhibited transition midpoints similar to that of the WT protein, suggesting stabilizing effects on their structures

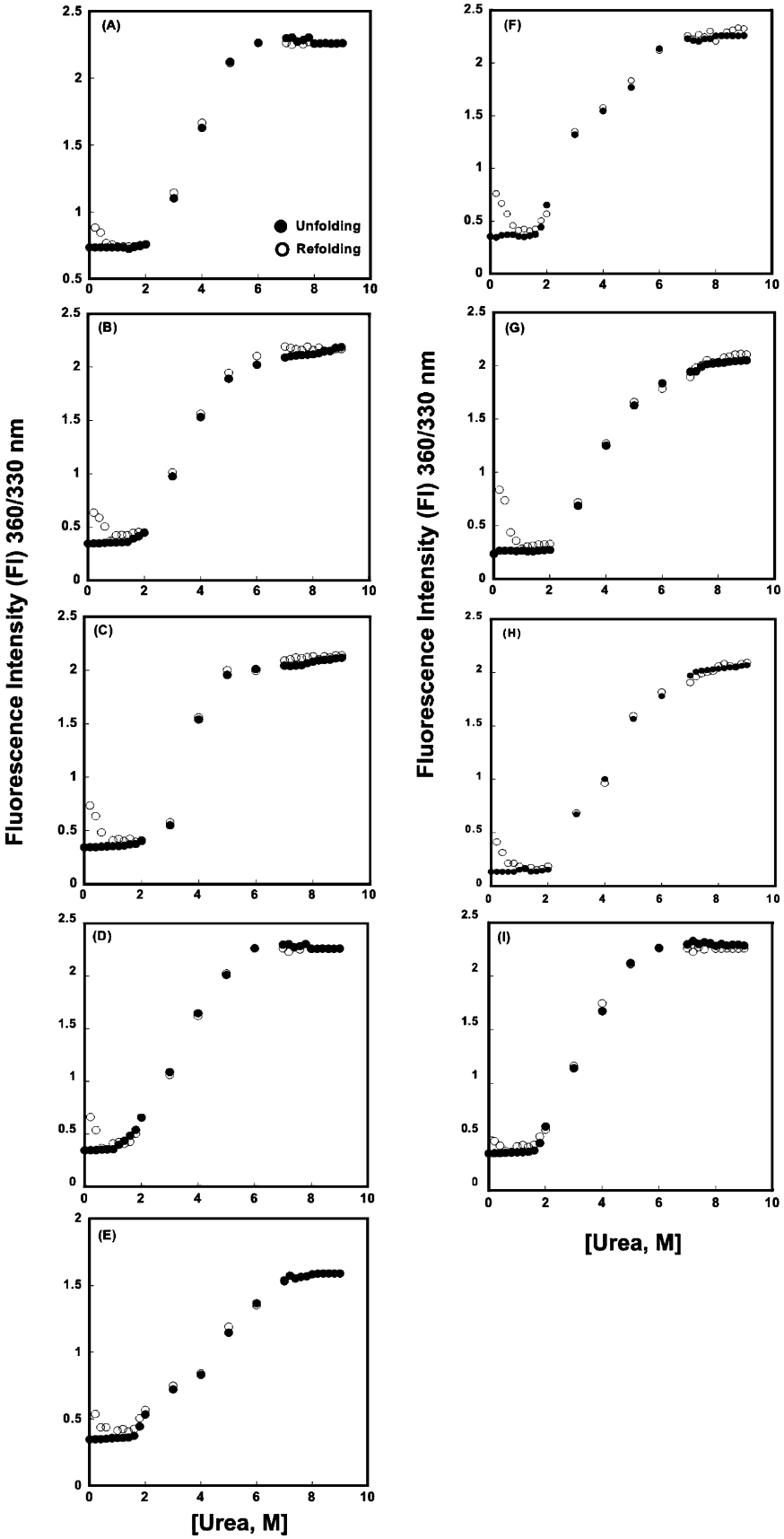

FIGURE 8: Equilibrium unfolding and refolding of WT βA3-crystallin and its eight truncated mutant proteins with urea as a denaturant. Proteins at 10 μg/mL in increasing concentrations of urea between 0 and 9 M in UR buffer were incubated at 37 °C for 24 h to ensure that equilibrium was reached. For the refolding experiments, different protein samples (100 μg) were denatured in 9 M urea in UR buffer for 24 h at 37 °C. The protein was subsequently refolded by dilution of proteins to 10 μg/mL at urea concentrations decreasing from 9 to 0.9 M: (A) WT protein, (B) βA3[21] mutant, (C) βA31[22] mutant, (D) βA3[N] mutant, (E) βA3[N+I] mutant, (F) βA3[N+I+II] mutant, (G) βA3[N+I+II+CP] mutant, (H) βA3[III+IV] mutant, and (I) βA3[IV] mutant.

Table 4: Equilibrium Unfolding−Refolding Transition Midpoints of WT βA3 and Its Deletion Mutant Proteins Using Urea as a Denaturant

	transition 1 (native to folding intermediate) midpoint (M)[a]	transition 2 (folding intermediate to unfolded) midpoint (M)[a]
WT βA3/A1	2.2	3.1
βA3[21]	1.5	3.1
βA3[22]	1.5	3.5
βA3[N]	1.4	3.2
βA3[N+I]	1.5	2.9
βA3[N+II]	1.8	2.8
βA3[N+II+CP]	1.5	3.1
βA3[III+IV]	2.7	4.4
βA3[IV]	2.5	4.2

[a] Molar concentration.

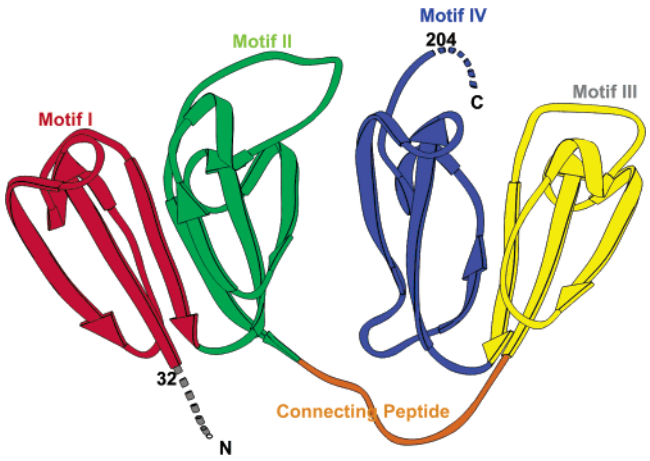

FIGURE 9: Three-dimensional structure of the monomer of βA3-crystallin. The model depicts the ribbon presentation of the N- and C-terminal domains and the location of all four Greek key motifs and the connecting peptide. The folding starts at residue 32 and ends at residue 204. The gray dashed line is the N-terminal extension, which is not involved in protein folding. Similarly, the blue dashed line, at the C-terminus, is also not involved in protein folding. The four motifs are colored differently: red for motif I, green for motif II, orange for connecting peptide, yellow for motif III, and blue for motif IV.

following truncation of 21 or 22 N-terminal amino acids or the entire N-terminal extension. On the basis of the existing literature and the proposed molecular model of βA3-crystallin (see Figure 9), the N-terminal extension (residues 1−30) is solvent exposed and does not contribute to protein conformation. Therefore, the existence of βA3-crystallin without 22 N-terminal residues in the newborn human (*41*) and our in vitro equilibrium data suggest potential stabilizing effects of the in vivo truncation on the structure of βA3-crystallin. Truncation of NTE and motifs I and II yielded lower transition unfolding midpoints, suggesting their destabilizing effects on the crystallin structure. Additional truncations at CP (i.e., βA3[N+I+II+CP] mutant) generated the C-terminal domain, and truncation of motifs III and IV (i.e., βA3[III+IV] mutant) generated the N-terminal domain (*36*). The C-terminal domain-containing mutant protein (βA3-[N+I+II+CP]) exhibited a transition midpoint (i.e., native to intermediate midpoint at 1.5 M and folding intermediate to unfolded midpoint at 3.1 M) lower than that of the protein containing the N-terminal domain (βA3[III+IV] mutant), which showed a "native to folding intermediate" midpoint of 2.7 M and a "folding intermediate to unfolded state" of 4.4 M. Together, the results suggest that the N-terminal domain is relatively more stable than the C-terminal domain. This difference also suggested independent unfolding and refolding of the two domains. Moreover, βA3[N+I+II+CP] mutants exhibited a decreased slope in the transition region, indicating fewer cooperations between unfolded and refolded intermediates (Figure 8G). Apparently, the removal of one globular domain from the βA3[III+IV] mutant might affect the overall stability by altering the domain−domain interface. The truncation of only motif IV resulted in similar reversible equilibrium unfolding and refolding spectra. However, both transitions were lower than that of the βA3 crystallin mutant, suggesting that truncation of motif IV alone results in a relatively less stable molecular structure. Together, the results suggested a lower stability of βA3-crystallin upon truncation of motifs III and IV.

DISCUSSION

The existing literature suggests that the two main initiating factors for age-related cataract development are post-translational modifications of crystallins and synthesis of defective crystallins due to genetic mutations. Both factors are shown to result in crystallin misfolding and unfolding and/or in altered interactions and association among native, modified, and defective crystallins leading to poorly soluble high-molecular mass aggregates. The major modifications of crystallins include oxidation, deamidation, and backbone truncation, which are believed to cause aggregation and insolubilization of crystallins during cataract development (*15*, *16*). Extensive post-translational truncations of β-crystallins with aging have been reported with their varying degrees of structural stability (*15*, *16*, *24*−*26*). Genetic mutations causing production of truncated βA3/A1-crystallin have been reported in autosomal dominant cataracts. For example, a 3 bp deletion in exon 4 in the βA3/A1-crystallin gene resulted in a deletion of G91 that produced truncated crystallin with impaired folding and solubility properties (*9*). Similarly, two separate splice site mutations in the CRYBA1/3 gene at exactly the same site resulted in cataracts with two different phenotypes (*11*, *41*).

The focus of our study was to compare the altered properties of βA3-crystallin following truncations of specific regions with the properties of the WT protein. The rationale was that truncations of specific regions in the crystallin, some of which naturally occur in vivo, would elucidate altered properties of truncated crystallins that could implicate their potential role in cataractogenesis. For this purpose, we generated eight deletion mutant βA3 proteins, starting the deletion from the N-terminal region (i.e., first 21 or 22 N-terminal residues or the entire N-terminal extension) followed by motif I, motif II, connecting peptide, motif III, and motif IV. The proteins with 22 N-terminal residues deletion, were included because such truncated βA3-crystallin species existed in vivo in lenses of a 4-day-old donor (*41*).

WT βA3-crystallin and the eight truncated mutant proteins were N-terminally tagged with six His residues, which facilitated their purification by Ni^{2+} affinity chromatography. We utilized the purified His-tagged proteins for various biophysical studies because the CD and fluorescence spectra of the WT protein were similar to those of a previously reported non-His-tagged WT βA3-crystallin (*33*). Further-

more, previous studies similar to ours have used His-tagged proteins to elucidate changes in the structural properties of mutant proteins relative to those of the WT protein [e.g., His-tagged βB2-crystallin (*14*) and His-tagged γD-crystallin (*34*, *40*, *42*)].

In contrast to the expression of WT βA3-crystallin in the soluble fraction of *E. coli* cells, the truncated mutant proteins were recovered either in the partially soluble form (i.e., βA3[21] mutant, βA3[22] mutant, βA3[N] mutant, and βA3[III+IV] mutant) or in the insoluble form in the inclusion bodies (i.e., βA3[N+I] mutant, βA3[N+I+II] mutant, βA3[N+I+II+CP] mutant, and βA3[IV] mutant) (Table 2). The truncations of either 21 or 22 N-terminal residues or the entire N-terminal extension (residues 1−30) only partially affected the solubility of the protein (i.e., protein present in both soluble and inclusion bodies). However, the deletion of the N-terminal domain [i.e., mutants with deleted N-terminal extension and motif I (residues 1−70), N-terminal extension and motifs I and II (residues 1−118), or N-terminal extension, motifs I and II, and connecting peptide (residues 1−123)] resulted in their insolubilization and recovery in the inclusion bodies. Additionally, the deletion of the C-terminal domain [mutants with deleted motifs III and IV (residues 124−215) or motif IV (residues 166−215)] resulted in either a partial loss of the solubility or insolubilization, respectively. Together, the results suggested that the contribution of the N-terminal extension is minimal in keeping the protein properly folded, but the deletion of either the N-terminal domain (motifs I and II) or the C-terminal domain (motifs II and IV) caused major structural instability, leading to their insolubilization. Further, because the deletion of motif IV resulted in recovery of an insoluble protein but the mutant with deleted motifs III and IV was partially soluble, motif IV apparently plays a critical role in keeping the protein properly folded via interaction with the N-terminal domain (motifs I and II). Our additional comparative studies of aging and cataractous human lenses showed selective insolubility of the truncated βA3-crystallin during aging and cataract development (ref *4* and unpublished results of O. P. Srivastava). Similarly, a βA3-crystallin species containing only the C-terminal globular domain (due to the loss of exons 3 and 4 in the mRNA of βA1) became water insoluble in an autosomal mutation (11). Because βA3-crystallin is progressively N-terminally cleaved in aging human lenses and cataract development, their potential insolubility might be important in cataract pathogenesis (*17*, *25*, *27*, *28*).

We determined the ANS binding and intrinsic fluorescence and CD spectral properties to probe and compare the structural properties of the mutant proteins with the WT species. ANS is an anionic fluorescent probe that binds to the apolar interface and exhibits a shift in the emission maxima due to changes in hydrophobic patches on protein misfolding (*44*). The ANS binding experiment showed two major effects in the mutant proteins compared to the WT protein (i.e., a decrease in the fluorescence and a red shift). Because the N-terminally truncated mutant proteins exhibited a decrease (quenching) in fluorescence with a red shift in the order βA3[21] < βA3[22] < βA3[N] (Figure 4), these proteins had less compact structures with smaller hydrophobic patches relative to the WT protein. The mutant proteins containing either only N- or C-terminal domains also exhibited a reduced level of ANS binding (indicated by fluorescence quenching) with the weakest binding in the protein with the N-terminal domain (i.e., mutant with motifs III and IV deleted). Additionally, except the βA3[III+IV] mutant protein, the other mutant proteins (i.e., βA3[N+I], βA3[N+I+II], βA3[N+I+II+CP], and βA3[IV]) exhibited a red shift suggesting that the proteins without an N-terminal domain formed relatively less compact structure with weaker hydrophobic patches than the WT protein. In contrast to these results, the mutant proteins with only the C-terminal domain showed significant quenching and no shift in λ_{max}, suggesting their anomalous structure.

The intrinsic Trp fluorescence spectral analyses under native and denaturing conditions of mutant proteins (Figure 6 and Table 3) further supported the ANS binding results. Three aromatic amino acids (Trp, Tyr, and Phe) are responsible for the total fluorescence of a folded protein, and most of the emission upon excitation at ∼295 nm is due to Trp residues. Trp when buried has an emission maximum near 320 nm, and if Trp is in a polar environment (i.e., surface-exposed), its emission maximum is near 350 nm. Human βA3/A1-crystallin contains a total of nine Trp residues (*33*), and among these, four Trp residues are buried (residues 73, 99, 168, and 198), three partially buried (residues 31, 96, and 195), and two exposed (residues 139 and 153). Therefore, each of the two domains of βA3-crystallin contains two buried Trp residues in the hydrophobic core, and their emission shifts could be used as a probe to monitor changes in the tertiary structures following truncations. A red shift was observed on deletion of either 21 or 22 residues of the N-terminal extension but not following deletion of the entire N-terminal extension (residues 1−30). Because Trp is absent in the N-terminal extension, there must be some interaction between the residues of the N-terminal extension and Trp to account for the observed red shift. With the deletion of residues 1−70 from the βA3[N+I] mutant protein, the partially buried Trp-31 was deleted and hence no red shift was observed, suggesting the microenvironment of the remaining eight Trp residues in the protein did not change. On further deletion of residues 1−118 (in the βA3[N+I+II] mutant protein) or 1−123 (in the βA3[N+I+II+CP] mutant protein), the partially buried Trp-31 and Trp-73 and buried Trp-96 were deleted, and this resulted in a red shift, suggesting that the microenvironment around the remaining Trp residues (at positions 139, 153, 168, 195, and 198) were altered. A similar result (a red shift) was also seen upon deletion of either residues 123−215 (in the βA3[III+IV] mutant protein) or residues 166−215 (in the βA3[IV] mutant protein). In the βA3[III+IV] mutant protein, Trp-153, Trp-168, Trp-195, and Trp-198 were deleted, and this resulted in an altered environment around the Trp residues at positions 31, 73, 96, 99, and 139. Similarly, the red shift in the βA3[IV] mutant protein suggested that the deletion of the Trp residues at positions 168, 195, and 198 resulted in changes in the microenvironment of the Trp residues at positions 31, 73, 96, 99, 139, and 153. Together, the results suggested that the deletions of motif II, III, or IV produced significant changes in the protein tertiary structure, whereas the changes due to deletion of the N-terminal extension and/or motif I were minimal. Further, the deletion of either N- or C-terminal domains of βA3-crystallin affected the secondary structure of the remaining molecule as assessed by CD spectra (Figure 5), which might be due to the disruption of

noncovalent interactions between the two domains. The molecular model (Figure 9) revealed that the two domains of βA3-crystallin are covalently joined by an extended linker and the side chains of amino acids interact noncovalently across the domain interface. The change in the hydrophobic cluster in the center of the interface between two domains might disrupt the pairwise interactions on the periphery of the hydrophobic cluster between the two domains and will presumably influence the folding, stability, and solubility of βA3-crystallin (*45*).

The results of ANS binding and Trp fluorescence emission of the truncated mutant proteins were further supported by their CD spectra (Figure 5). The proteins with truncation of up to the N-terminal extension exhibited spectra similar to that of WT βA3-crystallin, suggesting the presence of a β-sheet content of approximately 63%. This spectrum was similar to previously published spectra of native βA3/A1-crystallin (*9*, *33*) and that of β,γ-crystallins (*36*). The spectra have features in the range of 220−230 nm, which are believed to be due to Trp side chains (*46*). Upon the truncation of motifs I and II and CP (i.e., residues 1−123), the remaining polypeptide with the C-terminal domain exhibited spectra with a greater content of β-strand structure [73−75% vs the WT protein (63%)]. The spectra lacked a signal in the 220−230 nm region, which could be due to change in the hydrophobic cluster and tertiary structure because of the loss of two buried Trp residues (at positions 73 and 99) and two partially buried Trp residues (at positions 31 and 96). In contrast, upon truncation of motifs III and IV or only motif IV (residues 124−215), the remaining polypeptide with the N-terminal domain exhibited spectra with λ_{max} values between 205 and 208 nm, suggesting their largely unfolded structure, although they were not random coil compared to WT protein. These two mutant proteins also lacked two buried Trp residues (at positions 168 and 198) and one partially buried Trp residue (at position 195). Therefore, the C-terminal domain (motifs III and IV) was essential for a properly folded N-terminal domain of βA3-crystallin and might be involved in stabilizing the crystallin structure. The deleterious effect of the truncation of the C-terminal domain (motifs III and IV) on the structural stability of the N-terminal domain (motifs I and II) of βA3-crystallin is consistent with the results of ANS binding and their insoluble nature as described above. It has been reported that the deletion of G-91 resulted in relatively more unfolded polypeptide compared to WT βA3/A1 (*9*). Therefore, the genetic defect associated with human inherited cataract (*11*−*13*) and certain specific post-translational truncations might result in structural instability and defective folding of βA3/A1-crystallin and suggest a potential mechanism for protein aggregation and poor solubility seen in mature cataract.

The potential role of the N-terminal extension has been investigated previously (*17*, *47*, *49*). Upon removal of 30 residues of the N-terminal extension of mouse βA3/A1-crystallin, its dimer formation was affected (*47*). A ^{1}H NMR study following deletion of the first 22 amino acids of the N-terminal extension showed that the deleted segment was not involved in oligomerization (*48*). The loss of part of the N-terminal arm had no effect of the stability of βA3-crystallin; instead, the stability of the protein was slightly increased (*33*, *48*), which was also seen in our study. Another study further showed that the N-terminal arm of βB2-crystallin retained its flexibility in β_H- and β_L-complexes, but the arm of βA3/A1-crystallin was constrained (*49*). Further, the stability of N- and C-terminally cleaved rat βB2-crystallin was found to be lower than that of the full-length protein (*48*). Therefore, although the role of the N-terminal arm of βA3-crystallin is still unclear, our results suggest that the protein conformation is not significantly affected following deletion of the arm.

Because of the elusive role of N-terminal extension of βA3-crystallin during its interaction with other β-crystallins and the accumulation of the N-terminally truncated crystallin during aging and cataract development, it was important to explore the stability of the truncated mutant proteins by the equilibrium folding−unfolding studies. As in previous studies (*33*, *39*), we also used the Trp fluorescence as a probe to determine relative stabilities of WT and mutant proteins in the presence of varying concentrations of urea to obtain transition midpoints between native and unfolded states to rank their stabilities. This approach has shown that calf βB2 was relatively more stable than calf γB-crystallin (*36*), and this and previous studies have also shown the following rank order of stabilities of β,γ-crystallins: γS > βB1 > βA4 > βA1 > βA3 > βB2.

During equilibrium unfolding and refolding experiments, the transition midpoints of different truncated mutant proteins varied compared to that of the WT protein (Figure 8 and Table 4), which was due to stabilizing and destabilizing effects of specific truncations. Equilibrium unfolding−refolding analyses of the truncation of 21 or 22 N-terminal residues or the entire N-terminal extension showed minimal effects because their transition 2 midpoints were similar to that of the WT protein. On the basis of the similar transition midpoint analyses of the mutant proteins, it was concluded that the N-terminal domain of βA3 was relatively more stable than the C-terminal domain. The conclusion was also supported by the additional parameters determined by the biophysical methods described above. A recent report has shown that removal of the N-terminal extension of murine βA3/A1 increased the enthalpy and entropy significantly compared to those of the unmodified protein (*45*) and strengthened the tendency to dimerize compared to that of the WT protein.

On the basis of the molecular model proposed in Figure 9, the Prosite program suggested that the protein folding started at residue 32 and ended at residue 204, and the two domains were mostly β-sheet with slight α-helix structure. On the basis of the proposed structure, the N-terminal extension would be solvent-exposed without its participation in the three-dimensional conformation, which was consistent with our CD spectral results. The program also suggested that the truncation of motif IV would not only disrupt the noncovalent interactions with the N-terminal domain but also destabilize the C-terminal domain. Truncation of both motifs III and IV would result in the loss of the C-terminal domain and the disruption of the β-sheet structure as seen in our CD spectra (Figure 5). Because both N- and C-terminal domains are paired in a specific symmetrical manner around the hydrophobic interface, the truncation of either motif IV alone or both motifs III and IV would remove two buried Trp residues and one partially buried Trp. Also, these truncations exhibited maximum perturbation of the surface hydrophobicity and secondary and tertiary structures com-

pared to other truncations of the crystallin (Figures 4−6). Further, our results suggested that the truncation of both motifs III and IV would be relatively more deleterious as the three-dimensional domain pairing among β-crystallins is a prevalent hypothesis for their oligomerization (1). Also, homodimers of βA3 have been shown to exchange subunits to form hetero-oligomers with basic β-crystallins, which is more stable and more resistant to in vivo aggregation than the βA3-crystallin dimer (*33*). Such truncations are bound to hamper the oligomeric assembly in vivo, which is also important for maintaining high crystallin concentrations of 200−400 mg/mL in the human eye lens.

Our study presents results of deletion of different regions of βA3-crystallin when it is present as a homoaggregate. However, in vivo, except for βB2-crystallin which is present as a homodimer, other β-crystallins exist as heterodimers (*36*). For example, βB1 and βA3 spontaneously aggregate, and βA3/βB1 hetero-oligomers were found to be stable (*33*, *50*). Because the CD spectra of the β-crystallin heterooligomers suggest that their formation was accompanied by changes in secondary structure (*33*), the behavior of the deletion mutant protein under hetero-oligomer formation remains to be determined.

Truncation in βA3 leads to either premature termination of the polypeptide (*8*) or formation of only one domain (*11*). Also, deletion of a specific amino acid in βA3 resulted in defective folding and a reduction in solubility (*9*). Some of these studies have shown altered crystallin−crystallin interactions and conformational changes, which could lead to cataract development. Despite various truncations in α- and β-crystallins that lead to cataract formation, it remains unclear which conformations of crystallin are necessary for proper folding and oligomerization. Because these crystallins undergo various modifications, including truncation during aging, these may result in protein destabilization and unfolding into the aggregated forms, which apparently cause cataract formation. Previously, we have shown that βA3-crystallin undergoes primarily N-terminal truncation during aging (*27*). The present study showed that the loss of 21 and 22 amino-terminal amino acids and the N-terminal extension (βA3[21], βA3[22], and βA3[N] mutants, respectively) resulted in oligomerization (aggregates with masses of 259−267 kDa) but no changes in secondary structure; however, the loss of motifs III and IV (i.e., βA3[III+IV] and βA3[IV] mutants) resulted in significant changes in solubility properties, β-sheet structural content, and tertiary and quaternary structures. Further, the N-terminal domain (βA3[III+IV] mutant) is shown to be more stable than the C-terminal domain (βA3[N+I+II+CP] mutant). Therefore, the truncation of the N-terminal extension, which occurs at a very early developmental stage, does not significantly alter the structural properties. Also, the results suggested that locations of the truncations within βA3-crystallin are important in determining the solubility, stability, and oligomerizing properties.

ACKNOWLEDGMENT

We thank Martha Robbins for editorial assistance. We also thank Donald Muccio and Mike Jabalonski for technical assistance in recording the far-UV CD spectra in the Chemistry Department of the University of Alabama at Birmingham. The βA3-crystallin model was computed using coordinates from PDB entry 1BLB of βB1-crystallin with the help of Drs. Narayana Sthanam and Mike Carson of the Center for Biophysical Sciences and Engineering at the University of Alabama at Birmingham.

REFERENCES

1. Bloemendal, H., Zweers, A., Benedetti, E. L., and Walters, H. (1975) Selective reassociation of the crystallins, *Exp. Eye Res. 20*, 463−478.
2. Wistow, G., Turnell, B., Summers, L., Slingsby, C., Moss, D., Miller, L., Lindley, P., and Blundell, T. (1983) X-ray analysis of the eye lens protein γ-II crystallin at 1.9 Å resolution, *J. Mol. Biol. 170*, 175−202.
3. Hogg, D., Tsui, L. C., Gorin, M., and Breitman, M. L. (1986) Characterization of the human β-crystallin gene human βA3/A1 reveals ancestral relationships among the βγ-crystallin superfamily, *J. Biol. Chem. 261*, 12420−12427.
4. Harrington, V., McCall, S., Huynh, S., Srivastava, K., and Srivastava, O. P. (2004) Crystallins in water soluble-high molecular weight protein fractions and water insoluble protein fractions in aging and cataractous human lenses, *Mol. Vision 10*, 476−489.
5. Zarina, S., Zhao, H. R., and Abraham, E. C. (2000) Advanced glycation end products in human senile and diabetic cataractous lenses, *Mol. Cell. Biochem. 210*, 29−34.
6. Lapko, V. N., Cerny, R. L., Smith, D. L., and Smith, J. B. (2005) Modifications of human βA1/βA3-crystallins include S-methylation, glutathiolation, and truncation, *Protein Sci. 14*, 45−54.
7. Ueda, Y., Duncan, M. K., and David, L. L. (2002) Lens proteomics: The accumulation of crystallin modifications in the mouse lens with age, *Invest. Ophthalmol. Visual Sci. 43*, 205−215.
8. Burdon, K. P., Wirth, M. G., Mackey, D. A., Russell-Eggitt, I. M., Craig, J. E., Elder, J. E., Dickinson, J. L., and Sale, M. M. (2004) Investigation of crystallin genes in familial cataract, and report of two disease associated mutations, *Br. J. Ophthalmol. 88*, 79−83.
9. Reddy, M. A., Bateman, O. A., Chakarova, C., Ferris, J., Berry, V., Lomas, E., Sarra, R., Smith, M. A., Moore, A. T., Bhattacharya, S. S., and Slingsby, C. (2004) Characterization of the G91del CRYBA1/3-crystallin protein: A cause of human inherited cataract, *Hum. Mol. Genet. 13*, 945−953.
10. Graw, J., Jung, M., Loster, J., Klopp, N., Soewarto, D., Fella, C., Fuchs, H., Reis, A., Wolf, E., Balling, R., and de Angelis, H. (1999) Mutation in the βA3/A1-crystallin encoding gene Cryba1 causes a dominant cataract in the mouse, *Genomics 62*, 67−73,
11. Kanabiran, C., Rogan, P., Olmos, L., Basti, S., Rao, G. N., Kaiser-Kupfer, M., and Hejtmancik, J. F. (1998) Autosomal dominant zonular cataract with sutural opacities is associated with a splice mutation in the βA3/A1-crystallin gene, *Mol. Vision 4*, 18−21.
12. Santhia, S. T., Manisastry, S. M., Rawlley, D., Malathi, R., Anishetty, S., Gopinath, P. M., Vijayalakshmi, P., Namperumalsamy, P., Adamski, J., and Graw, J. (2004) Mutation analysis of congenital cataracts in Indian families: Identification of SNPS and a new causative allele in CRYBB2 gene, *Invest. Ophthalmol. Visual Sci. 45*, 3599−3607.
13. Litt, M., Carrero-Velenzuela, R., LaMorticella, D. M., Schultz, D. W., Mitchell, T. N., Kramer, P., and Maumenee, I. H. (1998) Autosomal dominant congenital cataract associated with a missense mutation in the human α crystallin gene CRYAA, *Hum. Mol. Genet. 7*, 471−474.
14. Liu, B.-F., and Liang, J. J.-N. (2005) Interaction and biophysical properties of human lens Q155* βB2-crystallin mutant, *Mol. Vision 11*, 321−327.
15. Hanson, S. R., Hasan, A., Smith, D. L., and Smith, J. B. (2000) The major in vivo modifications of the human water-insoluble lens crystallins are disulfide bonds, deamidation, methionine oxidation and backbone cleavage, *Exp. Eye Res. 7*, 195−207.
16. Ajaz, M. S., Ma, Z., Smith, D., and Smith, J. B. (1997) Size of human lens β-crystallin aggregates are distinguished by N-terminal truncation of βB1, *J. Biol. Chem. 272*, 11250−11255.
17. Werten, P. J., Lindner, R. A., Carver, J. A., and de Jong, W. W. (1999) Formation of βA3/βB2-crystallin mixed complexes: Involvement of N- and C-terminal extensions, *Biochim. Biophys. Acta 1432*, 286−292.

18. Lampi, K. J., Kim, Y. H., Bachimger, H. P., Boswell, B. A., Lindner, R. A., Carver, J. A., Shearer, T. R., David, L. L., and Kapfer, D. M. (2002) Decreased heat stability and increased chaperone requirement of modified human βB1-crystallins, *Mol. Vision 8*, 359−366.
19. Coop, A., Goode, D., Sumner, I., and Crabbe, M. J. (1998) Effects of controlled mutations on the N- and C-terminal extensions of chick lens beta B1 crystallin, *Graefe's Arch. Clin. Exp. Ophthalmol. 236*, 146−150.
20. Van Montfort, R. L. M., Bateman, O. A., Lubsen, N. H., and Slingsby, C. (2003) Crystal structure of truncated human βB1-crystallin, *Protein Sci. 12*, 2606−2612.
21. Shih, M., Lampi, K. J., Shearer, T. R., and David, L. L. (1998) Cleavage of β crystallins during maturation of bovine lens, *Mol. Vision 4*, 4−11.
22. Werten, P. J. L., Vod, E., and deJong, W. (1999) Truncation of βA3/A1-crystallin during aging of the bovine lens: Possible implications for lens optical quality, *Exp. Eye Res. 68*, 99−103.
23. Takemoto, L., Takemoto, D., and Brown, G. (1987) Antisera to synthetic peptides of MIP26K as probes of changes in opaque vs transparent regions within the same human cataractous lens, *Exp. Eye Res. 45*, 385−392.
24. Shearer, T. R., David, L. L., Anderson, R. S., and Azuma, M. (1992) Review of selenite cataract, *Curr. Eye Res. 4*, 357−367.
25. David, L. L., Lampi, K. J., Lund, A. L., and Smith, J. B. (1996) The sequence of human βB1-crystallin cDNA allows mass spectrometric detection of βB1 protein missing portions of its N-terminal extension, *J. Biol. Chem. 271*, 4273−4279.
26. Lampi, K. J., Ma, Z., Shih, M., Shearer, T. R., Smith, J. B., Smith, D. L., and David, L. L. (1997) Sequence analysis of βA3, βB3, and βA4 crystallins completes the identification of the major proteins in young human lens, *J. Biol. Chem. 272*, 2268−2275.
27. Srivastava, O. P., Srivastava, K., and Harrington, V. (1999) Age-related degradation of βA3/A1-crystallin in human lenses, *Biochem. Biophys. Res. Commun. 258*, 632−638.
28. Harrington, V., McCall, S., Huynh, S., and Srivastava, O. P. (2004) Crystallins in water soluble-high molecular weight protein fractions and water insoluble protein fractions in aging and cataractous human lenses, *Mol. Vision 10*, 476−489.
29. Ghosh, J. G., and Clark, J. I. (2005) Insights into the domains required for dimerization and assembly of human αB crystallin, *Protein Sci. 14*, 684−695.
30. Liu, B.-F., and Liang, J. J.-N. (2006) Domain interaction sites of human lens βB2-crystallin, *J. Biol. Chem. 281*, 2624−2630.
31. Gupta, R., and Srivastava, O. P. (2004) Deamidation affects structural and functional properties of human αA-crystallin and its oligomerization with αB-crystallin, *J. Biol. Chem. 43*, 44258−44269.
32. Laemmli, U. K. (1970) Cleavage of structural proteins during the assembly of the head of bacteriophage T4, *Nature 227*, 1680−1685.
33. Bateman, O. A., Sarra, R., van Genesen, S. T., Kappe, G., Lubsen, N. H., and Slingsby, C. (2003) The stability of human acidic β-crystallin oligomers and hetero-oligomers, *Exp. Eye Res. 77*, 409−422.
34. Flaugh, S. L., Kosinski-Collins, M. S., and King, J. (2005) Contributions of hydrophobic domain interface interactions to the folding and stability of human γD-crystallin, *Protein Sci. 3*, 569−581.
35. Jaenicke, R., and Slingsby, C. (2001) Lens crystallins and their microbial homologues: Structure, stability, and function, *Crit. Rev. Mol. Biol. 36*, 435−499.
36. Bloemendal, H., deJong, W., Jaenicke, R., Lubsen, N. C., Slingsby, C., and Tardieu, A. (2004) Ageing and vision: Structure, stability and function of lens crystallins, *Prog. Biophys. Mol. Biol. 86*, 407−485.
37. Basak, A., Bateman, O., Slingsby, C., Pande, A., Asherie, N., Ogun, O., Benedeck, G. B., and Pande, J. (2003) High-resolution X-ray crystal structures of human γD crystallin (1.25 Å) and the R58H mutant (1.15 Å) associated with aculeiform cataract, *J. Mol. Biol. 328*, 1137−1147.
38. Wieligmann, K., Mayr, E.-M., and Jaenicke, R. (1999) Folding and self-assembly of the domains of βB2-crystallin from rat eye lens, *J. Mol. Biol. 286*, 989−994.
39. Kim, Y. H., Kapfer, D. M., Boekhorst, J., Lubsen, N. H., Bachinger, H. P., Shearer, T. R., David, L. L., Feix, J. B., and Lampi, K. J. (2002) Deamidation, but not truncation, decreases the urea stability of a lens structural protein, βB1-crystallin, *Biochemistry 41*, 14076−14084.
40. Kosinski-Collins, M., Flaugh, S. L., and King, J. (2004) Probing folding and fluorescence quenching in human γD crystallin Greek key domains using triple tryptophan mutant proteins, *Protein Sci. 13*, 2223−2235.
41. Bateman, J. B., Geyer, D. D., Flodman, P., Johannes, M., Sileka, J., Walter, N., Moreira, A. T., Clancey, K., and Spence, M. A. (2000) A new locus for autosomal dominant cataract on chromosome 12q13, *Invest. Ophthalmol. Visual Sci. 41*, 3278−3285.
42. Kosinski-Collins, M., and King, J. (2003) In vitro unfolding, refolding, and polymerization of human γD crystallin, a protein involved in cataract formation, *Protein Sci. 12*, 480−490.
43. Kannabiran, C., Wawrousek, E., Sergeev, Y., Rao, G. N., Kaiser-Kupfer, M., and Hejtmancik, J. F. (1999) Mutation of βA3/A1 crystallin gene in autosomal dominant zonular cataract with sutural opacities results in protein with single globular domain, *Invest. Ophthalmol. Visual Sci. 40* (Suppl.), S786.
44. Musci, G., and Berliner, L. J. (1985) Probing different conformational states of bovine α-lactalbumin: Fluorescence studies with 4,4′-bis[1-(phenylamino)-8-naphthalenesulfonate], *Biochemistry 24*, 3852−3856.
45. Sergeev, Y. V., Wingfield, P. T., and Hejtmancik, J. F. (2000) Monomer−dimer equilibrium of normal and modified βA3-crystallins: Experimental determination and molecular modeling, *Biochemistry 39*, 15799−15806.
46. Woody, R. W. (1994) Contributions of tryptophan side chains to the far-ultraviolet circular dichroism of proteins, *Eur. Biophys. J. 23*, 253−262.
47. Hope, J. N., Chen, H. C., and Hejtmancik, J. F. (1994) βA3/A1-crystallin association: Role of the N-terminal arm, *Protein Eng. 7*, 445−451.
48. Werten, P. J. L., Carver, J. A., Janicke, R., and deJong, W. W. (1996) The elusive role of the N-terminal extension of βA3- and βA1-crystallin, *Protein Eng. 9*, 1021−1028.
49. Trinkl, S., Glockshuber, R., and Jaenicke, R. (1994) Dimerization of βB2-crystallin: The role of the linker peptide and the N- and C-terminal extensions, *Protein Sci. 3*, 1392−1400.
50. Bateman, O. A., Lubsen, N. H., and Slingsby, C. (2001) Association behaviour of human βB1-crystallin and its truncated forms, *Exp. Eye Res. 73*, 3211−3231.

BI060499V